AD-A107 601 NAVAL RESEARCH LAB WASHINGTON DC F/G 20/9
STEADY-STATE PLANAR ABLATIVE FLOW.(U)
NOV 81 W M MANHEIMER, D G COLOMBANT
UNCLASSIFIED NRL-MR-4644 NL

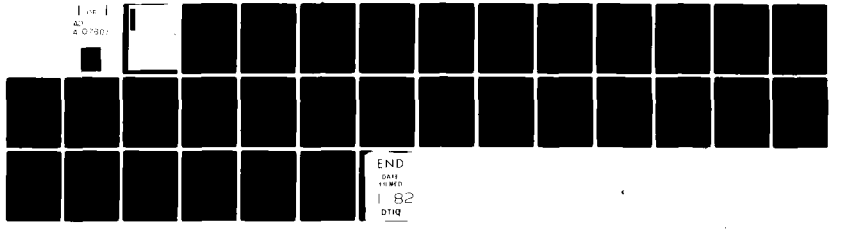

SECURITY CLASSIFICATION OF THIS PAGE (When Data Entered)

REPORT DOCUMENTATION PAGE		READ INSTRUCTIONS BEFORE COMPLETING FORM
1. REPORT NUMBER NRL Memorandum Report 4644	2. GOVT ACCESSION NO.	3. RECIPIENT'S CATALOG NUMBER
4. TITLE (and Subtitle) STEADY-STATE PLANAR ABLATIVE FLOW		5. TYPE OF REPORT & PERIOD COVERED Interim report on a continuing NRL Problem 6. PERFORMING ORG. REPORT NUMBER
7. AUTHOR(s) W. M. Manheimer, D. G. Colombant, and J. H. Gardner		8. CONTRACT OR GRANT NUMBER(s)
9. PERFORMING ORGANIZATION NAME AND ADDRESS Naval Research Laboratory Washington, D.C. 20375		10. PROGRAM ELEMENT, PROJECT, TASK AREA & WORK UNIT NUMBERS Sponsor Assignment No. DE-A108-79DP40092 J. O. 47-0859-0-1
11. CONTROLLING OFFICE NAME AND ADDRESS U. S. Department of Energy Washington, D.C. 20545		12. REPORT DATE November 18, 1981 13. NUMBER OF PAGES 31
14. MONITORING AGENCY NAME & ADDRESS(if different from Controlling Office)		15. SECURITY CLASS. (of this report) Unclassified 15a. DECLASSIFICATION/DOWNGRADING SCHEDULE

16. DISTRIBUTION STATEMENT (of this Report)

Approved for public release; distribution unlimited.

17. DISTRIBUTION STATEMENT (of the abstract entered in Block 20, if different from Report)

18. SUPPLEMENTARY NOTES

19. KEY WORDS (Continue on reverse side if necessary and identify by block number)

Laser produced plasma
Steady-state flow
Ablation flow
Nonuniform illumination
2D perturbation analysis

20. ABSTRACT (Continue on reverse side if necessary and identify by block number)

Steady state planar ablative flow in a laser produced plasma is studied. Our calculations relate all steady state fluid quantities to only three parameters, the material, absorbed irradiance and laser wavelength. The fluid is broken into three regions; the subcritical expanding plasma, the steady state ablation front and the accelerated slab. Boundary conditions at the interfaces of these regions are given. If the absorbed irradiance is nonuniform, the nonuniformity in ablation pressure is calculated. Results are compared with experiment and fluid simulation for both uniform and nonuniform illumination.

DD FORM 1 JAN 73 1473 EDITION OF 1 NOV 65 IS OBSOLETE
S/N 0102-014-6601

SECURITY CLASSIFICATION OF THIS PAGE (When Data Entered)

CONTENTS

STEADY-STATE PLANAR ABLATIVE FLOW

I. INTRODUCTION

There have recently been a series of experiments on laser driven ablative acceleration of thin foil targets at the Naval Research Laboratory[1-4] and elsewhere.[5,6] These experiments demonstrated acceleration of the foil up to speeds in excess of 10^7 cm/sec. The authors also compared the experimental results with a simple rocket model. The laser irradiances in these experiments are sufficiently low that plasma is most likely described by classical transport.

This paper discusses the theory of ablative acceleration. Since this problem can be solved in either one[7] or two[8] dimensions by fluid simulation, our principal object is not to find detailed solutions which can be compared precisely with experiment. Rather it is to shed light on the physics of ablative acceleration and to derive simple scaling laws. We do derive simple scaling laws for ablation pressure, blow-off velocity and separation between critical and ablation surfaces. These scaling laws depend only on the material, laser wavelength and absorbed laser irradiance. The key to deriving these simple scaling laws is not really in solving the steady state fluid equations, but rather in selecting which of many possible solutions describe the ablative acceleration.

Another crucial question for ablatively driven laser fusion is what degree of non-uniformity of illumination can be tolerated. Initial experiments in this area have also been done at the Naval Research Laboratory.[9,10] This paper also addresses the issue of non-uniform illumination.

The earliest theories of uniform laser driven acceleration assumed that the critical surface behaved like a Chapman-Jouguet deflagration point.[11-15] The dense, heated plasma then acts as a piston and drives a shock into the cold undisturbed fluid. The laser energy is ultimately coupled to the target by

Manuscript submitted August 20, 1981.

this shock wave. Except for Ref. 12, these theories neglect thermal conduction. They show that the ablation pressure P_4 scales as $I^{2/3}\lambda^{-2/3}$, and the blow-off velocity scales as $I^{1/3}\lambda^{2/3}$ where I is the absorbed irradiance and λ is the laser wavelength. They assume, as we do, that the laser light is absorbed only at the critical density. These scaling laws are similar to the ones we derive. This is interesting since thermal conduction is neglected. In ablative flow, thermal conduction is the principal inward energy transport mechanism.

More recent theories include the effects of thermal conduction.[16–20] These theories were done in either planar or spherical geometry. Since the thermal conduction is in fact very large in the blow-off plasma, we also include thermal conduction. In these newer theories, the scaling laws are either not explicitly given, or else they tend to be very complicated. For instance the scaling law for ablation pressure given in Ref. (19) is

$$P_4 = \left(I_0^{6/2 + M_s^2}\, \lambda^{-24}\, R_a^{2-M_s^2}\right)^{1/22+7M_s^2}$$

where M_s is the Mach number at which the thermal flux is inhibited, I_0 is the absorbed laser irradiance at the ablation surface and R_a is the ablation surface radius. Reference 18 finds on the other hand, that steady state solutions can only be found if their parameter M (proportional to critical-ablation surface separation in our theory) is between about 2/3 and 16/5. Also they find that steady state solutions exist at given critical to sonic density ratio, only for a particular value of absorbed irradiance, in other words the absorbed irradiance cannot be independently specified.

Our solutions are more like those calculated for planar geometry.[16,17] However the solutions presented here more clearly connect the flow to the laser parameters and show explicitly how the slab accelerates. In fact we find the acceleration is simply P_4/M where M is the mass of the slab which has *not* yet ablated away. Also the flow calculated in Refs. 16 and 17 require several more parameters to be specified. For instance solutions presented in Ref. 16 specify the temperature at the critical surface and acceleration whereas we solve for these. We need only specify the material, laser wavelength an absorbed irradiance. The calculations in Refs. 16 and 17 are also more difficult to apply to an experiment because fluid quantities are normalized to the values they have at the maximum density which is not known a priori.

We find that the fluid can most easily be described by breaking it into three regions. First there is the subcritical plasma which expands into a vacuum. Since it expands into a vacuum, it cannot be in a steady state; rather the expansion will be some sort of rarefaction wave. Since the thermal conduction is very high, an isothermal rarefaction is most reasonable.

Second there is the ablation front between the critical surface and the accelerated slab. We assume that the flow is in steady state there. The steady state ablation front can match smoothly to the nonsteady rarefaction if the isothermal Mach number is unity at the critical surface. This feature also corresponds to what is found in particle simulations[21] and theory[22] of laser light interaction with the critical surface. The analytic solution for fluid quantities in the ablation front tends to zero temperature a finite distance away from the critical surface. This point then marks the transition from the ablation front to accelerated slab. These two regions are described in Sec. II.

Third there is the accelerated slab itself. In Section III we review Kidder's theory[23] for an accelerated degenerate Fermi-Dirac gas. The structure near the transition point is almost impossible to calculate analytically since the material makes a transition there from degenerate Fermi gas to fully ionized plasma. In this work, we treat the transition as a contact discontinuity across which mass, momentum and energy flux are conserved, but do not concern ourselves with its detailed structure. Also we determine under what conditions the acceleration is negligible in the calculation of the properties of the ablation front.

In Section IV we examine the problem of non-uniform illumination. First, it is assumed that the one-dimensional flow pattern is stable so two-dimensional steady-state treatment is meaningful. If we assume all quantities have a small transverse perturbation, the steady state fluid equations can be linearized in the perturbed quantities. These linearized equations turn out to be a set of equations for an isothermal sound wave coupled to an equation for a thermal conduction wave. Approximate solutions to these equations are found which directly relate the non-uniformity of the absorbed irradiance to the non-uniformity of the ablation pressure at the slab. Since the acceleration of the slab is P_4 times the pulse time, we can simply derive velocity non-uniformity in terms of illumination non-uniformity.

In Section V we derive simple scaling laws for a laser produced plasmas and compare the theory with NRL experiments for both uniform and non-uniform illumination. Also we show that the one-dimensional solutions calculated are very close to what is found by one-dimensional numerical solution. As we will see, the theory compares reasonally well with experiment.

II. STEADY STATE ABLATION IN ONE DIMENSION

In this section, we examine the steady state flow which results when an intense laser beam illuminates a slab. The configuration is as shown in Fig. 1 with the laser on the right and the flow in the positive x direction. There are three distinct regions in the flow. Farthest to the right is the sub-critical density plasma. Since this plasma expands into a vacuum, it cannot be steady state; rather it will be characterized by some sort of rarefaction wave. Farthest to the left is the accelerating slab which we will discuss in the next section. In between is the region of steady state ablative flow. As we will see, and as has been pointed out by others,[16–20] the solution of the steady state fluid equations are quite straightforward. The main problem is to connect these solutions properly from one region to the next, so that one eliminates as many constants of integration as possible. We find the steady state ablative flows is characterized completely by the material, laser wavelength and absorbed laser irradiance.

In the reference frame in which the ablation front is at rest, the steady state conservation equations for mass and momentum are then

$$\frac{d}{dx}\rho v = 0 \tag{1a}$$

or

$$\rho v = \rho_c v_c \tag{1b}$$

and

$$\frac{d}{dx}(\rho v^2 + \rho T) = 0 \tag{2a}$$

or

$$\rho v^2 + \rho T = \rho_c v_c^2 + \rho_c T_c \tag{2b}$$

where ρ, v and T are the mass density, velocity and temperature. For convenience, the temperature has units of velocity squared, so that $T^{1/2}$ is the isothermal sound speed. A subscript c denotes the value of

a quantity at the critical density. Also we have neglected the ponderomotive force and the inertial force due to the accelerated reference frame. The former approximation is valid if the laser light energy denisty is small compared to the thermal energy density at the critical surface. We will discuss the validity of the latter approximation in the next section. The critical density ρ_c is determined by the material and laser frequency, (assuming the ion is fully stripped) but v_c and T_c are as yet undetermined. Equations (1 and 2 a) or (1 and 2 b) can be easily solved to give the following:

$$\frac{dv}{dx} = -\frac{1}{v(1 - T/v^2)} \frac{dT}{dx} \tag{3a}$$

or

$$\mathcal{M} = \frac{(v_c + T_c/v_c)/T^{1/2} \pm ((v_c + T_c/v_c)^2 T^{-1} - 4)}{2} \tag{3b}$$

where $\mathcal{M}$ is the isothermal Mach number $\mathcal{M} = v/\sqrt{T}$. Equation (3 a) shows that the flow becomes singular at the sonic point $\mathcal{M} = 1$. Thus the sonic transition cannot be in the region of steady state ablation.

If we assume that the thermal conduction is high, the expansion of the underdense plasma should be approximately described as an isothermal, rather than adiabatic, rarefaction wave. This (time dependent) solution is given by

$$\rho = \rho_c \exp(-x/T_c^{1/2} t) \tag{4a}$$

$$v = T_c^{1/2} + x/t \tag{4b}$$

where $x = 0$ corresponds to the critical density at all times. Clearly, this isothermal rarefaction wave can connect smoothly to the steady state ablative flow only if

$$v_c = T_c^{1/2}. \tag{5}$$

Thus as additional boundary condition for the ablative flow region, we assume the Mach number is equal to unity at the critical surface.

This choice is also compatible with other studies. First, it is known that the singularity at $\mathcal{M} = 1$ in the steady state fluid equations can be removed if the deposition of laser momentum at the critical surface is accounted for.[16,17] Lee et al[22] find that there is a density jump at the critical surface and the flow velocity makes a transition from subsonic on the high density side to supersonic on the low density

side. The density and velocity jump both approach zero as the electron oscillating velocity divided by electron thermal speed approaches zero. Actually there will be a small density jump at the critical surface but we do not consider it here. In the NRL ablation experiments, the laser irradiance is small enough that the ponderomotive force is unimportant. Secondly, as will be shown one dimensional fluid simulations in slab geometry do confirm that the isothermal Mach number is nearly always equal to about one at the critical surface. Thus Eq. (5) determines the velocity at the critical surface in terms of the temperature. The temperature will be determined from the energy equation.

Before turning to the energy equation, let us look at the expression for Mach number, Eq. (3 b). In the ablative flow region, the flow is subsonic. Also we expect that near the solid, the temperature will be small. Taking the subsonic solution of Eq. 3b for $\mathcal{M}$ in the limit of small T, we find

$$\mathcal{M} \approx T^{1/2}/2\,T_c^{1/2} \tag{6}$$

where we have used Eq. (5). Thus as the temperature decreases, so does the Mach number.

We now turn to the steady state energy equation which we write as

$$\frac{d}{dx}\left[\frac{5}{2}\,\rho v T - K T^{5/2}\,\frac{dT}{dx}\right] = I\delta(x) \tag{7a}$$

where I is the absorbed laser energy flux. Integrating in x for $x < 0$,

$$\frac{5}{2}\,\rho v T - K T^{5/2}\,\frac{dT}{dx} = S \tag{7b}$$

where S is the total constant energy flux. We have assumed the thermal conduction is proportional to $T^{5/2}$ as is appropriate for an ionized plasma. In Eq. (7) we have neglected the kinetic energy flux $1/2\,\rho v^3$ compared to the enthalpy flux $5/2\,\rho v T$. At the critical density, this is a 20% error. However as one approaches the solid, and $\mathcal{M}^2 = v^2/T$ decreases, this approximation gets better and better. Neglecting this term allows us to write a very simple analytic solution to the energy equation.

The next question is what the constant S is in Eq. (7 b). The individual terms on the left hand side of Eq. (7b) have roughly magnitude I, the laser irradiance. There are three possible physical effects which contribute to S. First it describes the heating (or preheat) of the slab. This contribution to S from the preheat is negative since in the configuration of Fig. 1 power travels from right to left to reach the slab.

Since accelerating targets with no preheat are of most interest to laser fusion, we do not consider preheat. Second there is the negative contribution to S from power deposited at the ablation surface needed to vaporize and ionize the slab. Since this energy is very small compared to flow and thermal energy, we neglect it also. Finally there is the power needed to accelerate the slab. This contribution to S is positive since in the reference frame of the ablation front the slab has positive velocity but negative acceleration. That is the slab loses energy. However the slab velocity is very small, being the critical velocity times the critical density divided by the solid density. Therefore we will also neglect the power coming out of the accelerated slab, so that $S = 0$ Eq. (7 b) becomes

$$\frac{5}{2}\rho v T - K T^{5/2}\frac{dT}{dx} = 0. \tag{7c}$$

Since ρv is constant, Eq. (7 c) has a simple analytic solution

$$T = \left[T_c^{5/2} + \frac{25}{4}\frac{\rho_c v_c}{K}x\right]^{2/5} \tag{8}$$

where $x = 0$ is assumed to be the critical surface. Notice that the equation is valid only for $x > -\frac{4}{25}\frac{K T_c^{5/2}}{\rho_c v_c}$, at which point it is singular in that $T \to 0$, but $\rho \to \infty$. (The solution for T versus x is plotted in Fig. 2). The problem now is to determine T_c and to determine the meaning of the singular behavior as $T \to 0$.

To find T_c we must examine the behavior of the flow near the critical density. Since we neglect ponderomotive force (i.e., laser momentum deposition), the density and velocity are continuous across the critical density. Since the thermal conduction is large, the temperature is also continuous across the critical density. The only discontinuous quantity then is the temperature gradient, and the discontinuity in it reflects the laser energy deposition at the critical density. Specifically

$$K T_c^{5/2}\left[\left.\frac{dT}{dx}\right|_0 - \left.\frac{dT}{dx}\right|_{0^-}\right] = I \tag{9}$$

where I is the absorbed laser irradiance. The question now is how much of this absorbed irradiance is conducted inward and how much is conducted outward.

The outward flux can be determined from the rarefaction wave solution, Eq. (4). The total flow energy flux, $\frac{1}{2}\rho v^3 + 5/2\rho v T$ through the critical surface is $3\rho_c V_c T_c$ where we have assumed $\mathcal{M} = 1$. However by integrating $\frac{1}{2}\rho v^2 + 3/2\rho T$ from $x = 0$ to ∞ and taking the time derivative, we find that the energy flux through $x = 0$ needed to drive the rarefaction is $4\rho_c V_c T_c$. Thus an additional energy flux $\rho_c V_c T_c$ must be supplied by outward thermal conduction so that

$$K T_c^{5/2} \left.\frac{dT}{dx}\right|_{x=0^-} = \rho_c v_c T_c. \tag{10}$$

Thus the temperature in the underdense plasma is not exactly constant. Our model for the rarefaction wave is valid in the limit $K \to \infty$ so that the relative temperature drop across this rarefaction wave is small. The inward flux can be obtained immediately from Eq. (9) and gives

$$K\ T_c^{5/2} \left.\frac{dT}{dx}\right|_{x=0} = \frac{5}{2}\rho_c v_c T_c. \tag{11}$$

Thus making use of $\mathcal{M} = 1$ the conditions at the critical surface are simply given by

$$K\ T_c^{5/2} \left.\frac{dT}{dx}\right|_{x=0} = \frac{5}{2}\rho_c T_c^{3/2} = \frac{5}{7} I. \tag{12}$$

The steady state ablative flow pattern is now determined by only three quantities, the material, the laser frequency and the absorbed irradiance.

To complete our specification of the flow, it is necessary only to describe the transition from solid to ablative flow. The mass flux is clearly conserved across this transition. The energy flux, which is zero is also conserved across this transition in the approximation that the convective part of the energy flux is zero. The problem is that the momentum flux $\rho v^2 + \rho T$ is discontinuous across this transition. The pressure then goes to accelerating the slab. The properties of the accelerated slab are discussed in the next section.

We now discuss briefly the transformation properties from the ablative flow to laboratory reference frame. One can show that the time dependent fluid equations are invariant to the Galilean transformation

$$
\begin{aligned}
v &\rightarrow v + V \\
x &\rightarrow x + Vt \\
t &\rightarrow t \\
T &\rightarrow T \\
Q &\rightarrow Q \\
g &\rightarrow g
\end{aligned}
\tag{13}
$$

where Q is the thermal energy flux and ρg is an inertial force density. Thus from the steady state solution in the ablation front reference frame, we can easily generate solutions in the laboratory frame, or any reference frame.

We digress briefly to consider the question of inhibited thermal conduction. First of all, we note that just inside the critical surface, the thermal energy flux is given by $5/2\rho_c v_c T$ and the energy flux decreases as one approaches the solid. Thus just by the nature of the steady state ablative flow with no preheat the electron thermal energy flux is limited to about $5/2\sqrt{\frac{m}{M}}$ times its free streaming value, where m and M are respectively the electron and ion masses. This value is in the range of flux limits which have often been quoted.[24] We emphasize that this flux limit has nothing to do with any microscopic physical process (for instance magnetic field or instability) which limits the electron thermal energy flux. Rather it has to do with the macroscopic properties of the fluid flow which is set up.

Now let us examine how different theories of flux limitation can affect these results. One theory is to say that the flux is either the classical value or $\propto \rho T^{3/2}$, whichever is less.[16,19,24] However if this is so, the only solutions to Eqs. (7) in the flux limited regime are ρ, v and T all equal to constants and the solution becomes indeterminate. In fact other authors have made this assumption and have found that parameters in the flux limited ablative flow region vary in space only because of the spherical divergence[19,20] or the acceleration of the slab.[16]

Another theory is to say that K in Eq. (7) is anomalously reduced. These theories at least relate Q to temperature gradient, which is certainly reasonable. Also theories relating Q to a particular instability generally have this feature.[25-28] If K is reduced by some factor f (but is still constant) then the

equations for fluid quantities can be solved exactly as before. The only difference is that the distance between the critical surface and solid is reduced by this same factor f. Thus if K is reduced, the steady state length scales are reduced by the same amount so that the thermal energy flux is unchanged. This effect has been seen in fluid simulations.[7]

To summarize, we have shown that the flow has three distinct regions, the undisturbed solid, the steady state ablative flow between solid and critical density, and the subcritical rarefaction wave. All aspects of the steady state flow (for instance temperatures, velocities, rate at which the solid is being eaten away) are determined by three parameters, the material, the laser wavelength, and the absorbed laser irradiance. If there is thermal flux limitation, it most likely manifests itself as a reduced separation between critical and solid density.

III. THE ACCELERATED SLAB

In this section we discuss the accelerated shell. First we review Kidder's[23] solution for the shell, and then we derive conditions for neglecting the effect of acceleration on the ablative flow. If all preheat is neglected the solid is assumed to be a degenerate Fermi gas so

$$P = \left[\left(\frac{\rho}{\rho_0}\right)^{5/3}\right] P_0 \tag{14}$$

where ρ_0 is the ambient density and P_0 is the ambient internal pressure of about 1 Mb (about 10^{12} dynes/cc). Since the gas is degenerate there is no thermal conduction. Assuming the kinetic part of the momentum flux is much less than P, the pressure gradient is just balanced by the inertial force so

$$\frac{dP}{dx} = -\rho g \tag{15}$$

where g is the acceleration of the slab. Integrating Eq. (15) across the slab we find

$$P_4 = -g\int \rho\, dx = -gM, \tag{16}$$

P_4 is the ablation pressure at the surface of the slab given by Eq. (2b) and M is the total mass of the slab. We re-emphasize that P_4 is determined entirely by the material, laser wavelength and absorbed irradiance. Equation (16) then gives the acceleration in terms of the mass of the slab. If $x = x_0$ is the position of zero density at the front of slab

$$\frac{\rho}{\rho_0} = \left[\frac{2}{5}\,\frac{\rho_0 g}{P_0}\,(x_0 - x)\right]^{3/2} \tag{17}$$

where in our configuration $g < 0$ and $x_0 - x < 0$. The upper density boundary of the slab is just determined by the total mass of the slab. To the right of this upper boundary is the region of ablative flow. For our purposes here we regard this transition as a contact discontinuity across which mass, momentum and energy flux are conserved. The actual nature of this transition is extremely complicated because material goes from a Fermi degenerate gas to a fully ionized plasma. Thus, Eqs. (7) are not able to treat this transition region in either steady or non steady flow.

The next question is what effect the acceleration has on the ablative flow region. To account for the acceleration, one adds a term $-\rho g$ and $-\rho v g$ to the right hand sides of Eqs. (2 a) and (7 a). Thus, crudely speaking, acceleration is negligible if $g << \frac{dT}{dx}$. According to Eq. (8), T goes from the critical temperature to zero in a distance $4KT_c^{5/2}/25\rho_c v_c$ so the effect of acceleration on the ablative flow is negligible if

$$\frac{4gKT_c^{3/2}}{25\rho_c v_c} << 1. \tag{18}$$

where T_c is given by Eq. (12) and v_c is related to T_c by the Mach one condition.

IV. THE EFFECT ON NON-UNIFORM ILLUMINATION

A crucial question for laser fusion driven by ablative acceleration is what degree of non uniformity of illumination can be tolerated. The slab is ultimately accelerated by the total pressure at the ablation surface $\rho_4 v_4^2 + \rho_4 T_4 \approx \rho_4 T_4$, so we are interested in determining the non-uniformity of pressure at the ablation surface in terms of nonuniformity of laser irradiance. In order to do so within the context of the steady state fluid equations, it is necessary to assume that the flow pattern is stable. If a perturbation is set up at the critical surface, the steady state fluid equations show that this perturbation will either grow or decay as one moves away from the critical surface. If the flow pattern is stable, these growing perturbations represent fluctuations initialized elsewhere and decaying toward the critical surface. Thus for perturbations initialized at the critical surface, the proper boundary conditions for the assumed stable flow pattern is to consider only perturbations which decay away from the critical surface.

We will scale the equations so the dependent and independent variables are $\theta = \rho/\rho_c$, $\nu = v/|v_c|$, $\tau = T/T_c$ and $\chi = x/x_0$ where $x_0 = KT_c^2/\rho_c$. In terms of the scaled variables, the solution for temperature, Eq. (8) becomes

$$\tau = \left[1 + \frac{25}{4}\chi\right]^{2/5} \tag{19}$$

so that the separation between χ_c and χ_A is 0.16. It is now assumed that all quantities are the x dependent solutions described in Section II plus a small transverse perturbation proportional to exp *iky*. The steady state fluid equations are then linearized in the small perturbations to give

$$\frac{d}{d\chi}\tilde{S} + k\,\theta\,\nu_c\tilde{\nu}_c = 0 \tag{20}$$

$$\frac{d\tilde{J}}{d\chi} + k\theta\tilde{\nu}_c = 0 \tag{21}$$

$$\theta\nu_c\frac{d}{d\chi}\tilde{\nu}_c - \frac{k\tau}{\nu_c^2 - \tau}(2\bar{J}\nu_c - \tilde{S}) = k\theta\cdot\frac{\nu_c^2}{\nu_c^2 - \tau}\tilde{\tau} \tag{22}$$

$$\frac{d^2\tilde{\tau}}{d\chi^2} - \frac{10\theta\nu_c}{\tau^{5/2}}\frac{d\tilde{\tau}}{d\chi} - k^2\tilde{\tau} = \frac{5}{2}\frac{d\tau}{d\chi}\tilde{J} \tag{23}$$

where in writing Eqs. (20)-(23), we have changed notation slightly by redefining $i\nu_c \to \nu_c$ so that each equation is real. A tilde superscript indicates a perturbed quantity. Also we have used as dependent variables $\tilde{S}$ and $\tilde{J}$ instead of $\tilde{\theta}$ and $\tilde{\nu}_c$. The quantity $\tilde{J}$ is the perturbed mass flux in the x direction

$$\tilde{J} = \tilde{\theta}\nu_c + \theta\tilde{\nu}_c \tag{24}$$

and $\tilde{S}$ is the perturbed xx component of the total momentum flux tensor (the perturbed ablation pressure)

$$\tilde{S} = \tilde{\theta}(\nu_c^2 + \tau) + 2\theta\nu_c\tilde{\nu}_c + \theta\tilde{\tau}. \tag{25}$$

Equation (20) is the x component of the momentum equation, Eq. (21) is the mass equation, Eq. (22) is the y component of the momentum equation, and Eq. (23) is the temperature equation. In writing the latter, we have made use of Eq. (20) to eliminate several terms. It is precisely $\tilde{S}_4$ which we want to relate to the nonuniformity in laser irradiance.

It is clear that Eqs. (20-23) are singular at the isothermal sonic point $\nu_c^2 = \tau$. Also the first three equations are coupled to the last one through the right hand sides of Eqs. (22) and (23). This coupling and singular behavior make the decaying solutions difficult to find.

To get a useful result on the behavior under non-uniform illumination, as well as to gain insight into the physical processes taking place, we neglect this coupling; that is we set the right hand sides of Eqs. (22) and (23) equal to zero. We will come back and discuss this shortly.

Thus the equations describing the steady state fluctuating quantities are Eqs. (20) and (21) and

$$\theta \nu_x \frac{d}{d\chi} \tilde{\nu}_y - \frac{k\tau}{u^2 - \tau} (2\tilde{J}\nu_x - \tilde{S}) = 0 \tag{26}$$

$$\frac{d^2\tilde{\tau}}{d\chi^2} - \frac{10\,\theta\nu_x}{\tau^{5/2}} \frac{d\tilde{\tau}}{d\chi} - k^2\tilde{\tau} = 0. \tag{27}$$

Equation (27) above is the thermal conduction equation, the middle term being the effect of the fluid flow. Assuming that $\tilde{\tau} \sim \exp \int K dx$, the zeroth order WKB solution for the local dispersion relation is

$$K_T = \frac{5\theta\nu_x}{\tau^{5/2}} \pm \left[\frac{25\,\theta^2\nu_x^2}{\tau^5} + k^2 \right]^{1/2} \tag{28}$$

so the two values of K_T are real and have opposite sign. This is the thermal wave, but coupled to the ambient fluid flow. For $k \lesssim \frac{5\,\theta\,\nu_x}{\tau^{5/2}}$, the flow has a very strong effect on the thermal wave. Equations (20), (21) and (26) are simply the equations for isothermal sound waves in a flowing system. The local dispersion relation is

$$K_s^2 = \frac{k^2\tau}{\tau - \nu_x^2}. \tag{29}$$

Equation (29) is just the dispersion relation for isothermal sound wave $(\omega - k_x\nu_x)^2 - k^2\tau = 0$ where $\omega = 0$ and k_x is pure imaginary. Since $\tau > \nu_x^2$ in the underdense plasma, K_s^2 also has two real roots, one positive and one negative. The sound wave damps at zero frequency because it is cut off, like an electromagnetic perturbation in a waveguide below the cut off frequency. Although Eq. (29) appears to be singular at $\tau - \nu_x^2 = 0$, the integrated amplification, $\exp \int_0^{\tau=\nu_x^2} K_s\,dx$ is well behaved and bounded.

If a pure thermal wave is set up in the plasma, $\tilde{S}$, $\tilde{J}$ and $\tilde{u}_1$ are all zero. However since $\tilde{S}$ depends on the $\tilde{\tau}$ initially set up fluctuations in $\tilde{\theta}$ and $\tilde{\nu}_1$ are generated. In other words, a pure thermal wave cannot generate a pressure gradient or mass flow. On the other hand, if a pure isothermal cut-off sound wave is generated, $\tilde{\tau} = 0$.

The solutions to the uncoupled equations which decay away from the critical surface are then easy to find. These should be reasonably good approximations to the solution to the coupled set as long as $K_T \neq K_s$ at each point in the flow pattern. An examination of Eqs. (28) and (29) shows that for all k, $K_T = K_s$ at some point in the flow. However if k is small, the point where $K_T = K_s$ is very close to the critical surface. For instance, if $kx_0 < 16$, the density at this point is between ρ_c and $1.1\,\rho_c$. If we assume that the flow pattern has a slight jump at the critical density,[21,22] then the uncoupled equations should be a good approximation to the perturbed flow pattern for sufficiently small k.

The problem now is to solve Eqs. (20), (21), (26) and (27) for a region of steady ablative flow illuminated by a non-uniform laser beam and find the solutions which decay away from the critical surface. If the absorbed laser irradiance is $I + \tilde{I}$, then according to Eq. (12),

$$\frac{\tilde{\tau}}{\tau} = \frac{2}{3}\,\frac{\tilde{I}}{I}. \tag{30}$$

This temperature perturbation decays away from the critical surface according to the solution of Eq. (27). In the WKB approximation it decays away with K_T given by Eq. (28) with the positive sign chosen, since the critical surface is at $x = 0$ and the overdense plasma is at negative x.

The next question is what pressure non-uniformity, $\tilde{S}$, at the critical surface is generated by the laser irradiance non-uniformity. Since this pressure nonuniformity decays away from the critical surface with local decay rate given by Eq. (29), one can easily calculate that for the decaying cut off sound wave near the critical surface $\tilde{\theta}_c = -\,\tilde{\nu}_{xc}/\tau_c$ so that $\tilde{S}_c = \theta_c\,\tilde{\tau}_c + (1 - \nu_{xc}^2/\tau_c)\,\tilde{v}_{xc}$. Since the flow at the critical surface is assumed to be sonic, we have the result

$$\tilde{S}_c = \theta_c\,\tilde{\tau}_c = \frac{2}{3}\,\theta_c\,\tau_c\,\frac{\tilde{I}}{I}. \tag{31}$$

The fluctuating pressure then decays away from the critical surface according to the solution of Eqs. (20), (21) and (26). A plot of $\tilde{S}_4/\tilde{S}_c$ versus kx_0, from the numerical solutions of these equations is shown as the solid curve in Fig. 3. Also shown in Fig. 3 as the dashed curve is the simple result $\tilde{S}_4/\tilde{S}_c = \exp(-\,.16\,kx_0)$ given by Brueckner.[29] This is the solution to the thermal conduction equation with no flow, $\nabla^2\tau = 0$ and assuming pressure fluctuations follow temperature fluctuations. Our calculations show somewhat more smoothing of pressure fluctuations in the ablation front. Clearly there is a

great deal of smoothing of the pressure fluctuation for $kx_0 \gtrsim 8$. Also, as is apparent from Eqs. (28) and (29), for small k, the thermal wave damps out very quickly in the overdense plasma where $\tau << 1$, whereas the damping rate of the cut off sound wave is not strongly affected by low temperature. Thus near the ablation surface, the thermal wave should have much smaller amplitude than the cut-off sound wave; that is there should be small temperature perturbation.

V. APPLICATION TO A LASER PRODUCED PLASMA AND COMPARISONS WITH ONE-DIMENSIONAL FLUID SIMULATION

In this section, we apply the theory developed in the previous three sections to laser produced plasmas and compare with experiment and fluid simulation. If T_e represents the electron temperature, and equipartition is assumed then the total thermal pressure is $(1 + Z)\rho\ T_e$ (ergs)$/M_i$ where M_i is the ion mass and Z is the charge state. The ion mass is the atomic number A times the proton mass. Then the quantity T in Eq. (2), the isothermal sound speed squared is

$$T = \frac{(1 + Z)}{M_i}\ T_e \text{ (ergs)}. \tag{32}$$

From the expression for electron thermal conduction in an unmagnetized plasma,[30] we find that the quantity K in Eq. (7) is

$$K = \frac{3.7 \times 10^{-33}\ A^{7/2}}{(1 + Z)^{7/2}\ Z_{ei}\ \Lambda} \tag{33}$$

where

$$Z_{ei} = \frac{\sum_\alpha Z_\alpha^2\ n_\alpha}{\sum_\alpha Z_\alpha\ n_\alpha}, \tag{34}$$

the effective Z for collisional processes, and Λ is the Coulomb logarithm. There are several predictions of the one dimensional theory which give rise to simple scaling laws and/or which can be compared with experiment. These are the ablation pressure, blow-off velocity, distance from critical to ablation surface, and condition for neglect of acceleration in the ablation front. The ablation pressure is $2\rho_c\ T_e$, assuming Mach one flow at the critical surface. For a CH target used in the NRL experiments, $Z = 3.5$, $A = 6.5$, $Z_{ei} = 5$, $\rho_c = 3 \times 10^{-3}$ and we assume $\Lambda = 5$. In this case, using Eq. (12) to related temperature to absorbed irradiance, we find

$$P_A = 2\rho_c T_c = 2.6 \times 10^{12} \left(\frac{I}{10^{13}}\right)^{2/3} \lambda^{-2/3} \text{ dynes/cm}^2$$

$$= 2.6 \times \left(\frac{I}{10^{13}}\right)^{2/3} \lambda^{-2/3} \, Mb \tag{35}$$

where I is the absorbed laser irradiance in W/cm^2 and λ is the wavelength in microns. Notice that there is an advantage in going to shorter wavelengths. Assuming that the absorbed irradiance is 80% of the incident irradiance, the scaling law given by Eq. (35) is plotted in Fig. 4, along with points taken from the NRL experiment.[3] Clearly the agreement is very good, particularly as Eq. (35) is an absolute scaling law with no phenomenological constants.

The next quantity of interest is the expansion velocity. The quantity most accessible to theory is the velocity at the critical density which for the plastic target is

$$v_c \approx 2 \times 10^7 \left(\frac{I}{10^{13}}\right)^{1/3} \lambda^{2/3} \text{ cm/sec.} \tag{36}$$

The quantity most accessible to experimental measurement is the velocity far from the critical surface. The magnitude of this velocity is greater than v_c, but just how much greater depends on how far away the measurement is, and just when the approximation of a one dimensional isothermal rarefaction wave breaks down (this might be determined for instance by the spot size). In Fig. 5 is shown the scaling law given by Eq. (36) as well as measurements from the NRL experiment.[4] The actual velocity is about 2.5 times greater than given by Eq. (36), but the scaling agrees very well.

We now consider the distance between the ablation surface and critical surface. According to Eq. (19), this is .16 times the distance x_0 where

$$x_0 = \frac{K T_c^2}{\rho_c} = 350 \left[\frac{I}{10^{13}}\right]^{4/3} \lambda^{14/3} \text{ microns.} \tag{37}$$

At long wavelength, the scale lengths expand very rapidly. For example, a CO_2 laser produced plasma at 10^{13} W/cm^2 has a critical to ablation spacing of several meters. Clearly, these long scale length plasma can never form in a laser fusion experiment. Thus, if the thermal transport is classical, the behavior of a CO_2 laser produced plasma is dominated by its transient response and will not reach

steady state. However if the transport is inhibited, then the length scales can be reduced. Thus while short wavelength has the advantage of increasing ablation pressure at given irradiance, long wavelength has the advantage of increasing the critical to ablation surface separation so that nonuniformities in laser irradiance can be smoothed out before they reach the ablation surface.

The next question is the condition for the neglect of the acceleration on the blow-off plasma. Equation (18) reduces to

$$10^{-17}\, g \left[\frac{I}{10^{13}}\right]^{2/3} \lambda^{10/3} \ll 1. \tag{38}$$

For accelerations of order 3×10^{15} cm/sec^2 as measured in Ref. 1 and 2, the effect on the blow-off plasma is negligible up to irradiance of order 10^{15} W/cm^2 and higher.

We now discuss experiments with non-uniform laser illumination.[9,10] In Ref. 10 a portion of the laser light was masked out causing an intensity minimum at the center of the laser spot. The ratio intensity at the dip to maximum intensity was 1 : 2, 1 : 6 and 1 : 10 and the wavelength (peak to peak separations) took on values of 280 μ or 440 μ. The velocity non-uniformity of the accelerated target is then measured as a function of irradiance. We compare here the results of that experiment to the linear theory developed in Section IV. Since that theory is linear in non-uniformity, we compare only with the experiment having the 2 : 1 irradiance ratio. This experiment had a 280 μ transverse wavelength.

The velocity fluctuation should be proportional to the fluctuation in pressure at the ablation surface times the pulse time. Therefore

$$\frac{v_{MAX} - v_{MIN}}{v} = \frac{2\tilde{S}_4}{S_4}. \tag{39}$$

The quantity $\tilde{S}_4$ is related to $\tilde{S}_c$ by the graph in Fig. 6. Then, as in Sec IV, $\tilde{S}_c = \frac{2}{3}\rho_c T_c (\tilde{I}/I)$. Making use of the fact that x_0 is given by Eq. (37), we find that $v_{MAX}/v_{MIN} - 1$ versus irradiance is given by Fig. 6. Also shown on Fig. 6 are experimental points taken from Ref. 10. Clearly there is very reasonable agreement.

As a check on some of the one-dimensional theory derived here, we have also performed a number of one-dimensional fluid simulations in planar geometry. The code, described elsewhere[7] is modified only by eliminating inverse bremsstrahlung absorption and by depositing all absorbed laser energy at the critical surface. This is in agreement with the theoretical model described in Section II. To test the scaling of parameters on wavelength and irradiance for a plastic target, we have performed five simulations with parameters given in Table 1. The parameters are as given for the CH target except that Z_{eff} was taken as 3.5 instead of 5. According to Eq. (37), this would make x_0 of the simulation larger by a factor 10/7. First, we point out that all simulations in the table did come to a steady state in that the separation between critical surface and ablation surface did approach a constant value, with both surfaces moving into the accelerated slab. The third column of the table shows the isothermal Mach number at the critical density in the reference frame of the ablation front. Clearly this Mach number is very near unity. The worst agreement was in the second row where the Mach number was very difficult to measure due to large acceleration of the slab. Approximate power law formulae for the ablation pressure and critical to ablation surface separation are

$$P_a \sim I^{.6}\lambda^{-.6}$$
$$x_0 \sim I^{1.2}\lambda^{1.3}.$$

These formulae have scaling very nearly as given in Eqs. (35) and (37). However as is apparent from other one dimensional simulations,[7] the complicating effects of inverse bremsstrahlung absorption and spherical geometry can cause significant changes in these scaling laws. In all simulations however, the separation between critical and ablation surface is a very rapidly increasing function of laser wavelength.

Table 1

λ (μ)	I (W/cm^2)	$\mathcal{M}$	P_a (Mbar)	0.16 x_0 (μ)
0.53	10^{15}	0.97	4.3	4.4
0.53	10^{14}	0.8*	16.0	60
1.06	10^{15}	0.94	0.6	4.7
1.06	10^{15}	0.88	2.5	80
2.7	10^{15}	1.	0.3	236

*Isothermal Mach number at critical surface was very difficult to measure due to the large acceleration of the slab

ACKNOWLEDGMENTS

Many useful discussions with Dr. S. Bodner are acknowledged. This work was supported by the Department of Energy.

REFERENCES

1. R. Decoste, S.E. Bodner, B.H. Ripin, E.A. McLean, S.P. Obenschain and C.M. Armstrong, Phys. Rev. Lett. **42**, 1673 (1979).

2. B.H. Ripin, R. Decoste, S.P. Obenschain, S.E. Bodner, E.A. McLean, F.C. Young, R.R. Whitlock, C.M. Armstrong, J. Grun, J.A. Stamper, S.H. Gold, D.J. Nagel, R.H. Lehmberg and J.M. McMahon, Phys. Fluids **25**, 1012 (1980).

3. J. Grun, R. Decoste, B.H. Ripin and J. Gardner, NRL Memorandum Report 4410 (1981).

4. B.H. Ripin, S.E. Bodner, S.H. Gold, R.H. Lehmberg, E.A. McLean, J.M. McMahon, S.P. Obenschain, J.A. Stamper, R.R. Whitlock, F.C. Young, H.R. Griem, J. Grun, and M.J. Herbst, NRL Memorandum Report 4212 (1980).

5. M.H. Key, R.G. Evans, P.T. Rumsby, W. Toner, Topical meeting on Inertial Confinement Fusion, San Diego (1980).

6. H. Nishimura, H. Azechi, K. Yamada, A. Tamura, Y. Inada, F. Matsuoka, M. Hamada, Y. Suzuki, S. Nakai and C. Yamanaka, Phys. Rev. A **23**, 2011 (1981).

7. J.H. Gardner, and S.E. Bodner, NRL Memorandum Report (to be published).

8. M.H. Emery, J.H. Gardner, J.P. Boris, and J.H. Orens, NRL Memorandum Report 4500 (1981).

9. S.P. Obenschain, R.H. Lehmberg and B.H. Ripin, Appl. Phys. Lett. **37**, 903 (1980).

10. S.P. Obenschain, B.H. Ripin, E.A. McLean, and J. Grun, NRL Memorandum Report 4466 (1981).

11. C. Fauguignon and F. Floux, Phys. Fluids **13**, 386 (1970).

12. J.L. Bobin, Phys. Fluids **14**, 2341 (1971).

13. R.E. Kidder, Nucl. Fusion **8**, 3 (1968).

14. A. Caruso and R. Gratton, Plasma Phys. **10**, 867 (1968).

15. K. Nozaki and K. Nishihara, J. Phys. Soc. Japan **48**, 993 (1980).

16. F.S. Felber, Phys. Rev. Lett. **39**, 84 (1977).

17. J.H. Orens, NRL Memorandum Report 4167 (1980).

18. S.J. Gitomer, R.L. Morse and B.S. Newberger, Phys. Fluids **20**, 234 (1977).

19. C.E. Max, C.F. McKee and W.C. Mead, Phys. Fluids **23**, 1620 (1980) and Phys. Rev. Lett. **45**, 28 (1980).

20. C. Max, R. Fabbro and E. Fabre, Bull. Am. Phys. Soc., **25**, 895 (1980).

21. D. Forslund, J.M. Kindel, K. Lee, E.L. Lindman, and R.L. Morse, Phys. Rev. A **11**, 679 (1975); D. Biskamp and H. Welter in Plasma Physics and Controlled Nuclear Fusion (International Atomic Energy Agency, Vienna, 1974), Vol. II p. 507, J. DeGroot and J. Tull, Phys. Fluids **18**, 672 (1975); K.G. Estabrook, E.J. Valeo and W.K. Kruer, Phys. Fluids **18**, 1151 (1975).

22. K. Lee, D.W. Forslund, J.M. Kindel and E.L. Lindman, Phys. Fluids **20**, 51 (1977).

23. R.E. Kidder, Nucl. Fusion **19**, 223 (1979).

24. R.C. Malone, R.L. McCrory and R.L. Morse, Phys. Rev. Lett. **34**, 721 (1975).

25. W.M. Manheimer, Phys. Fluids **20**, 265 (1977).

26. W.M. Manheimer, C.E. Max, and J. Thomson, Phys. Fluids **21**, 2009 (1978).

27. S.P. Gary, J. Plasma Phys. **21**, 361 (1979).

28. S.P. Gary and J. Sanderson, Phys. Fluids **24**, 638 (1981).

29. K.A. Brueckner and S. Jorna, Rev. Mod. Phys. **46**, 325 (1974).

30. S.L. Braginskii, in *Reviews of Plasma Physics*, edited by M.A. Leontovich (Consultants Bureau, New York, 1966), Vol. 1, p. 205.

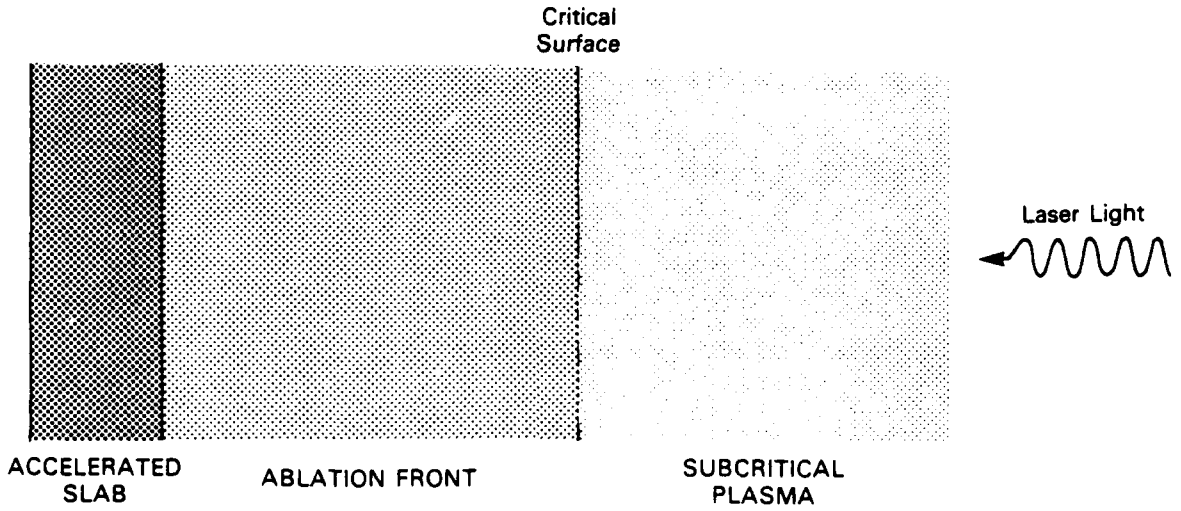

Fig. 1 — Configuration for ablative acceleration

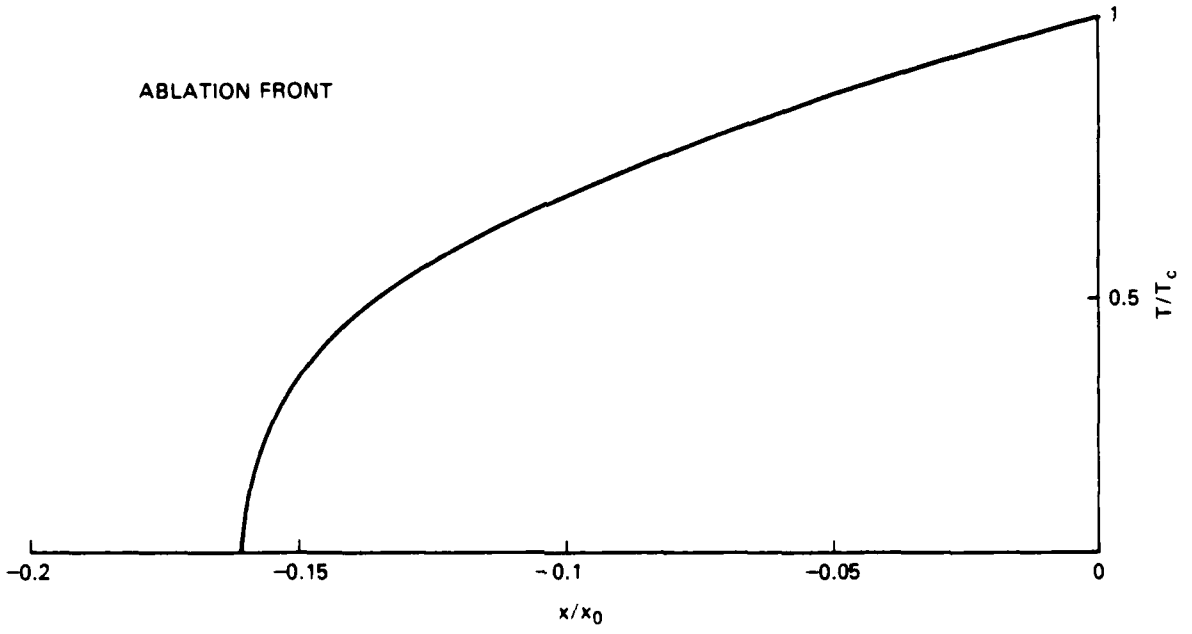

Fig. 2 — Relative temperature profile in the ablation front

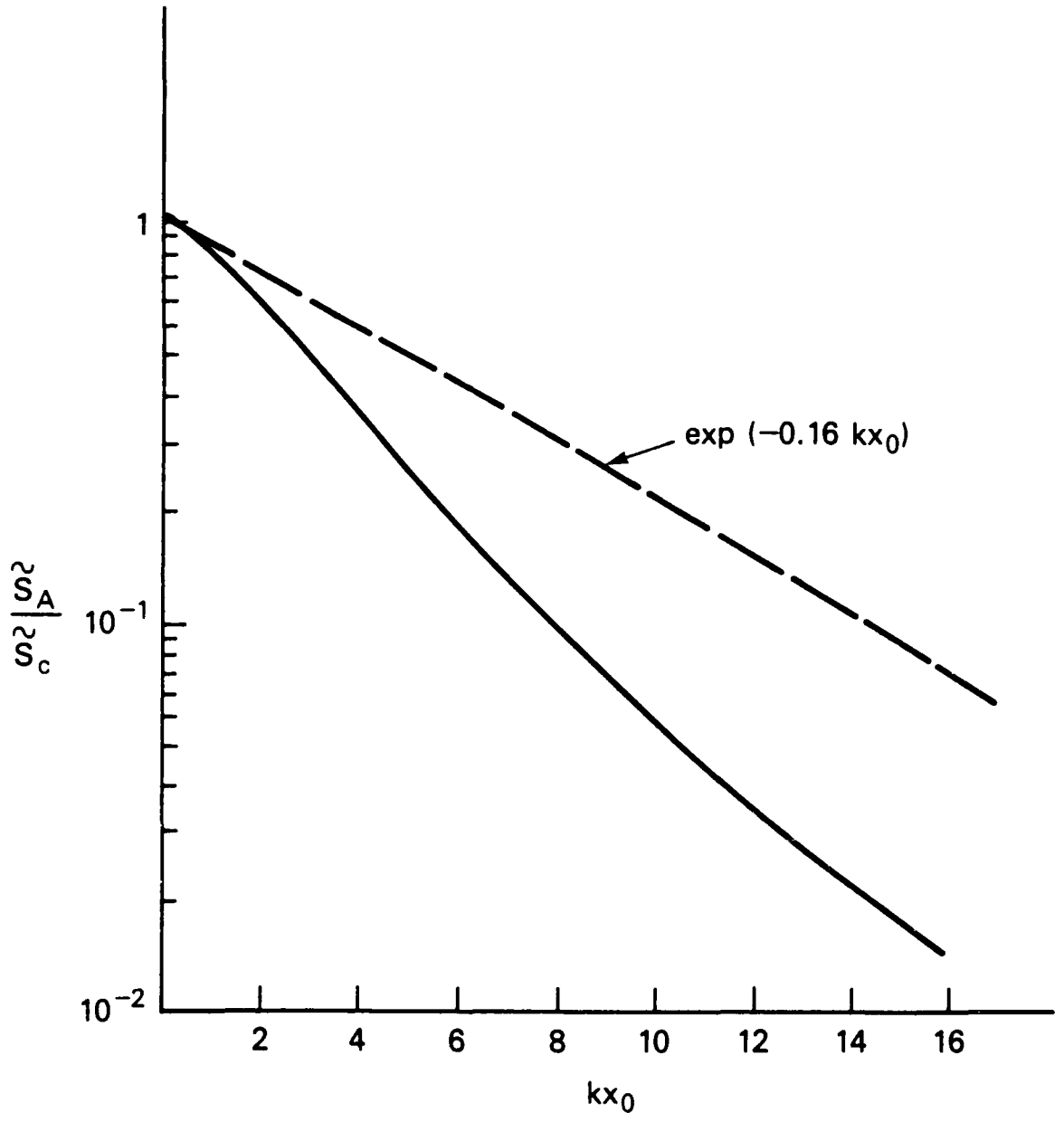

Fig. 3 — Ratio of the ablation pressure at ablation surface to the ablation pressure at critical surface ------ Same ratio for simple theory of Ref. 29 ------

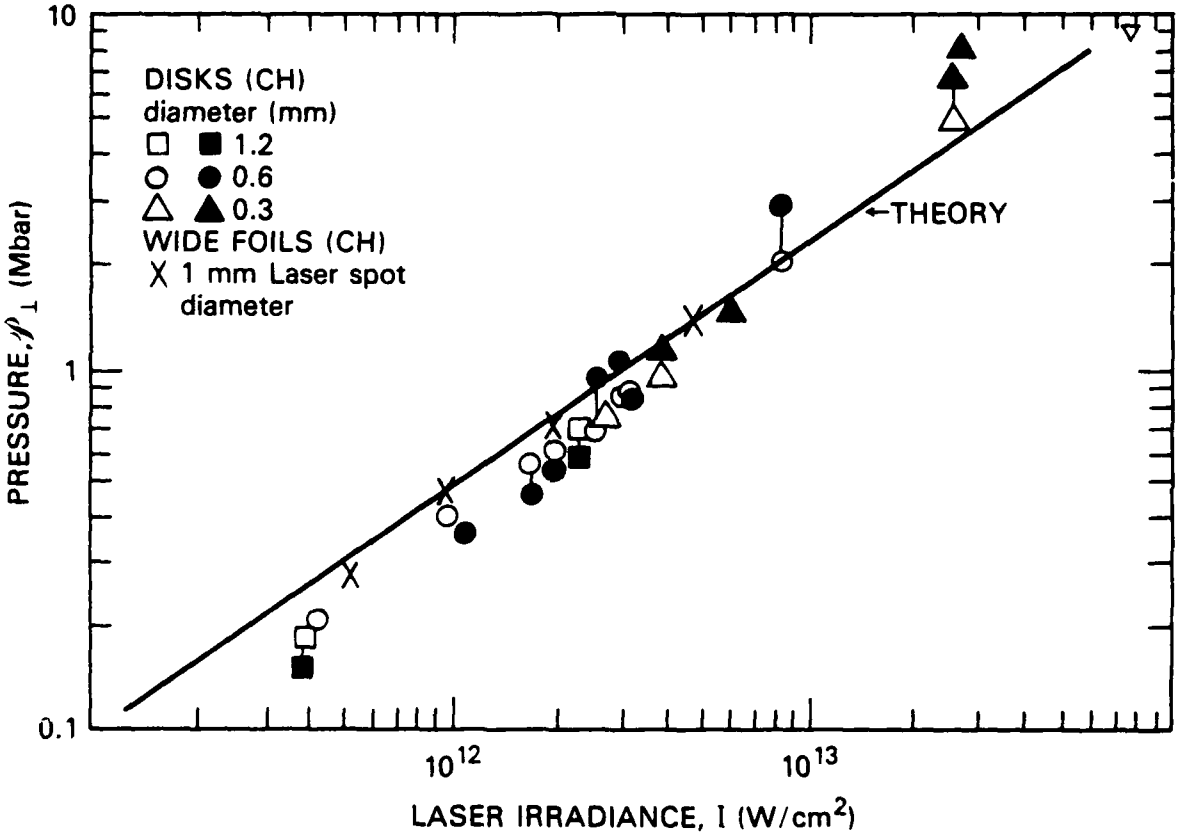

Fig. 4 — Comparison of measured ablation pressure to theory

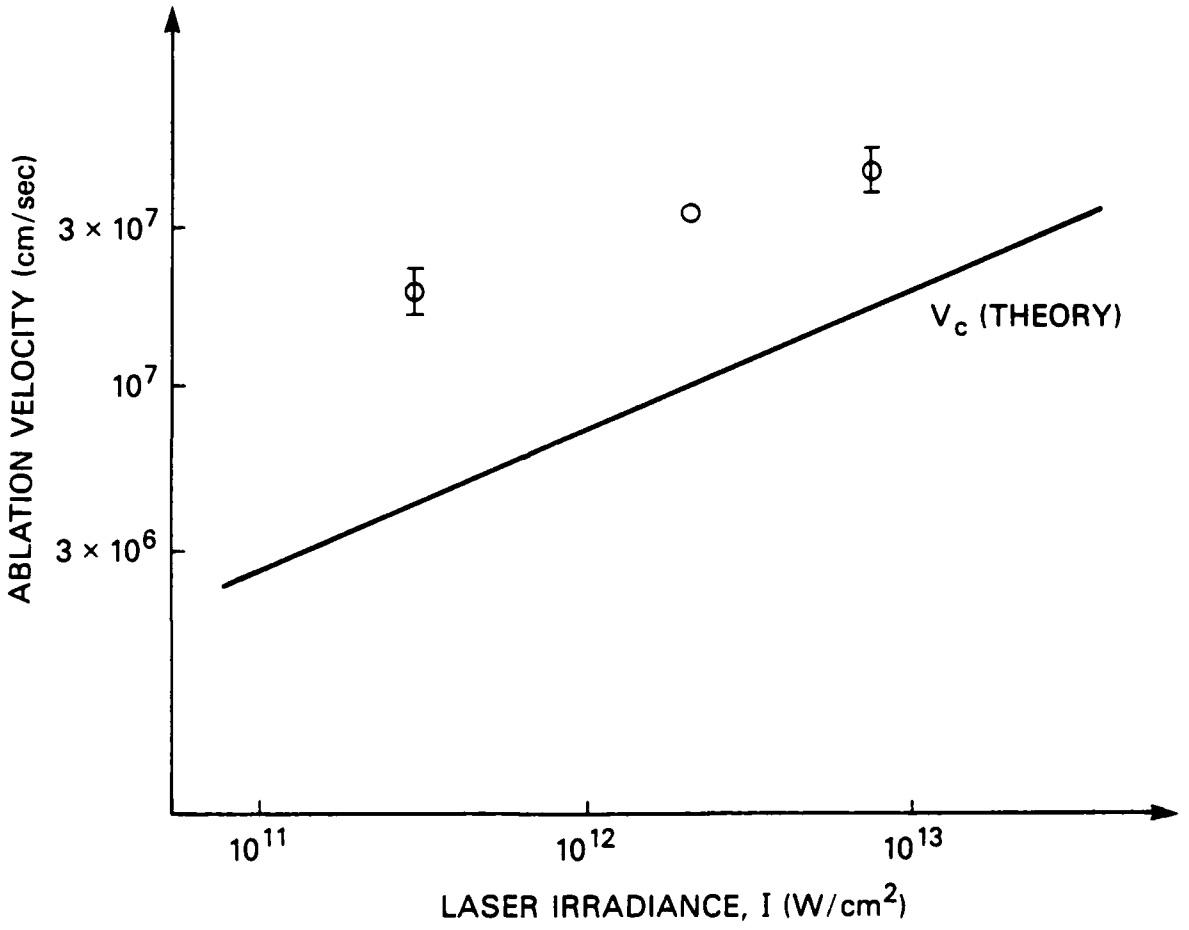

Fig. 5 — Comparison of measured velocity far from target with calculated velocity at the critical surface

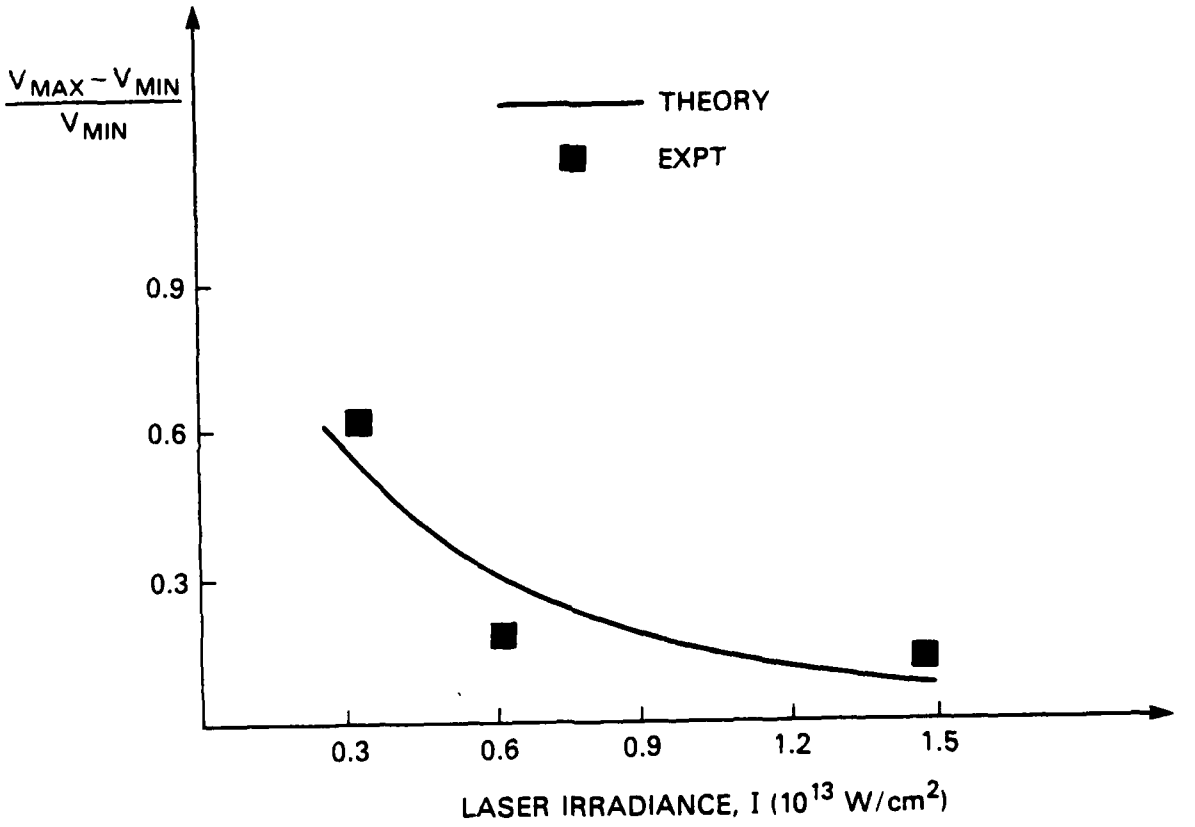

Fig. 6 — Comparison of calculated values of $\Delta v/v$ with nonuniform illumination experimental values

DISTRIBUTION LIST

USDOE (50 copies)
P.O. Box 62
Oak Ridge, TN 37830

National Technical Information Service (24 copies)
U.S. Department of Commerce
5285 Port Royal Road
Springfield, VA 22161

NRL, Code 2628 (35 copies)

NRL, Code 4790 (100 copies)

NRL, Code 4700 (26 copies)

USDOE (6 copies)
Office of Inertial Fusion
Washington, D.C.
Attn: Dr. G. Canavan
Dr. R. Schriever
Dr. S. Kahalas
Dr. T. Godlove
Dr. K. Gilbert

Lawrence Livermore National Lab.
P.O. Box 808
Livermore, CA 94551
Attn: Dr. D. Attwood, L481
Dr. W. Kruer, L545
Dr. B. Lasinski
Dr. C. Max, L545
Dr. A. Glass
Dr. L. Coleman
Dr. J. Nuckolls
Dr. W. Mead
Dr. N. Ceglio
Dr. R. Kidder

Department of Physics and Astronomy
University of Maryland
College Park, MD 20740
Attn: Dr. H. Griem

Los Alamos National Scientific Lab.
Los Alamos, NM 87545
Attn: Dr. R. Godwin
Dr. D. Giovanielli
Dr. J. Kindel
Dr. D. Forslund

University of Rochester
Rochester, NY 14627
Laboratory for Laser Energetics
Attn: Dr. R. S. Craxton
Dr. W. Seka
Dr. R. McCrory

KMS Fusion
3941 Research Park Drive
P.O. Box 1567
Ann Arbor, MI 48106
Attn: Dr. F. Mayer

Institut fur Plasmaphysik
8046 Garching
Bei Munchen
West Germany
Attn: Dr. R. Sigel
Dr. H. Takabe c/o Dr. P. Mulser

National Research Council
Division of Physics
100 Susser Drive
Ottawa K1A-0R6, Canada
Attn. Dr. J. Alcock

University of Quebec
INRS Energie
Case Postale 1020
Varennes, Quebec
Attn: Dr. T. Johnston
Dr. R. Decoste
Dr. H. Pepin

Sandia National Laboratory
Albuquerque, NM
Attn: Dr. K. Matzen
Dr. J Anthes
Dr. R. Palmer

Institute for Laser Engineering
Osaka University
Suita Osaka, 565
Japan
Attn: Dr. C Yamanaka
Dr. K. Nishihara
Dr. Mima
Dr. Yabe

Shanghai Institute of Optics and Fine Mechanics
Academia Sinica
Shanghai, PRC
Attn: Prof. Gan Fu-xi
Prof. Yu Wen-yan
Prof. Xu Zhi-zhan
Prof. Deng Xi-ming
Prof. Tan Wei-han
Mr. Pan Cheng-min

Soreq Nuclear Center
Yavne, Israel
Attn: Dr. A. Krumbein

Sergio Morosi
Ist. Fisica Applicata
via Bassi 6 Pavia - ITALY

Defense Technical Information Center
Cameron Station
5010 Duke Street
Alexandria, VA 22314

Prof. G. Wallis
Prof. Klaus Junge
Zentralinstitut fur Optik und Spektroskopie
DDR-1199 Berlin-Adlershof
Rudower Chaussee 6
West Germany

N. Kovalsky
Kurchatov Institute of Atomic Energy
D-182 Moscow
USSR

Rutherford Laboratory
Chilton, Didcot
Oxon OX110QX
England
Attn: Dr. M. Key
Dr. R. Evans

J. Balmer
Institute of Applied Physics
Sidlerstr. 5
CH-3012 BERN/Switzerland

Hn Qiguan
Lab. de Physique des Lasers
Uni. Paris Nord
93430 Villetaneuse/FRANCE

Gl. Barifi
Istituto Fisica Application
Universita di Paria
Pavia 27100
Italy

N.A. Tahir
Dept. of Nat. Phil
Glasgow University
Glasgow G12 (U.K.)

HDE
CEL
BP27
94190 Villeneuve St. Georges
FRANCE
Attn: Dr. M. Decroisette
DR. B. Meyer
Dr. A. Decoster
Dr. J. Kupersztych

D. Unaugst
University of Jena
6900 Jena
Schlobgassel
Germ. Dem. Rep.

Patrick Flynn
Bldg. N78
Atomic Weapons Research Estab
Aldermaston
Reading, U.K.

Ecole Polytechnique Greco ILM
Palaiseau 91127
FRANCE
Attn: Dr. E. Fabre
Dr. R. Fabbro
Dr. J. Virmont

INTERNAL DISTRIBUTION

Code 4730 Dr. S. Bodner
Dr. B. Ripin
Dr. E. McLean
Dr. J. Stamper
Dr. S. Obenschain
Dr. M. Herbst
Dr. R. Lehmberg

Code 4040 Dr. J. Boris
Dr. M. Emery